Accepted Manuscript

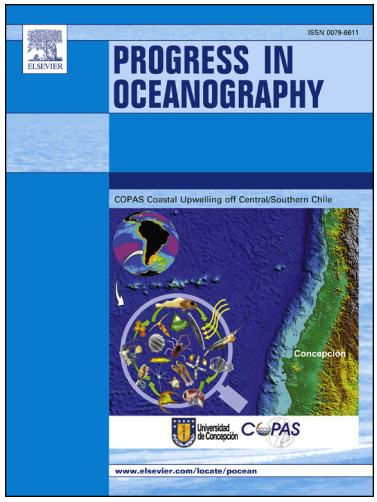

Effects of lower trophic level biomass and water temperature on fish communities: A modeling study

Jérôme Guiet, Olivier Aumont, Jean-Christophe Poggiale, Olivier Maury

PII: S0079-6611(15)30036-7
DOI: http://dx.doi.org/10.1016/j.pocean.2016.04.003
Reference: PROOCE 1703

To appear in: *Progress in Oceanography*

Received Date: 18 October 2015
Revised Date: 13 April 2016
Accepted Date: 13 April 2016

Please cite this article as: Guiet, J., Aumont, O., Poggiale, J-C., Maury, O., Effects of lower trophic level biomass and water temperature on fish communities: A modeling study, *Progress in Oceanography* (2016), doi: http://dx.doi.org/10.1016/j.pocean.2016.04.003

Effects of lower trophic level biomass and water temperature on fish communities : A modeling study

Jrme Guiet[a,b], Olivier Aumont[c], Jean-Christophe Poggiale[d], Olivier Maury[a,b]

[a] *IRD (Institut de Recherche pour le Dveloppement) - UMR 248 MARBEC, Av Jean Monnet CS 30171, 34203 Ste cedex, France*
[b] *University of Cape Town, Dept. of Oceanography - International Lab. ICEMASA Private Bag X3, Rondebosch 7701, Cape Town, South Africa*
[c] *IRD (Institut de Recherche pour le Dveloppement) - LOCEAN - IPSL, place Jussieu, 75252 Paris Cedex 05, France*
[d] *University Aix-Marseille - UMR 7294 MIO - OCEANOMED - Bt. Mditerrane, LUMINY, 163 Avenue de Luminy, case 901, 13009 Marseille, France*

Abstract

Physical and biogeochemical changes of the oceans have complex influences on fish communities. Variations of resource and temperature affect metabolic rates at the individual level, biomass fluxes at the species level, and trophic structure as well as diversity at the community level. We use a Dynamic Energy Budget-, trait-based model of the consumers' community size-spectrum to assess the effects of lower trophic level biomass and water temperature on communities at steady state. First, we look at the stressors separately in idealized simulations, varying one while the second remains constant. A multi-domain response is observed. Linked to the number of trophic levels sustained in the consumers' community, the regimes highlighted present similar properties when lower trophic level biomass is increased or temperature decreased. These trophic-length domains correspond to different efficiencies of the transfer of biomass from small to large individuals. They are characterized by different sensitivities of fish communities to environmental changes. Moreover, differences in the scaling of individuals' metabolism and prey assimilation with temperature lead to a shrinking of fish communities with warming. In a second step, we look at the impact of simultaneous variations of stressors along a mean latitudinal gradient of lower trophic level biomass and temperature. The model explains known observed features of global marine ecosystems such as the fact that larger species compose

fish communities when latitude increases. The structure, diversity and metabolic properties of fish communities obtained with the model at different latitudes are interpreted in light of the different trophic-length domains characterized in the idealized experiments. From the equator to the poles, the structure of consumers' communities is predicted to be heterogeneous, with variable sensitivities to environmental changes.

Keywords : Community size-spectrum ; Dynamic Energy Budget ; Biodiversity ; Bergmann's rule ; Trait based model ; Marine ecosystem model ; Impact of the environment ; Latitudinal gradient ; Ecosystem regimes.

Introduction

Climate driven physical and biogeochemical changes impact marine ecosystems properties in a number of ways (Bindoff et al. (2007) ; Doney et al. (2012)). They affect individuals directly, modifying their access to resources through increased stratification (Sarmiento et al. (2004) ; Bopp et al. (2013)) or their metabolism through temperature changes (Gillooly et al. (2001) ; Clarke & Fraser (2004)), acidification (Fabry et al. (2008)) or de-oxygenation (Prtner & Knust (2007)). These direct effects at the individual level propagate to the community level through alterations of the biomass transfer across trophic and organization levels. For example, climate change has been shown to induce a global body size shrinking (Daufresne et al. (2009) ; Sheridan & Bickford (2011)). It will also lead to changes in community level fish production (Blanchard et al. (2012) ; Lefort et al. (2015)) or biodiversity (Cheung et al. (2009)). These indirect responses modify the services provided by marine ecosystems. Fisheries are expected to be particularly affected and the consequences in terms of food security and economic profitability are major issues (Brander (2007) ; Jennings & Brander (2010)). In this context, understanding the intricate response of fish communities to environmental changes is an urgent challenge (Rice & Garcia (2011) ; Merino et al. (2012)).

However, investigating and modeling environmental effects on fish communities is a difficult task, the environment acts directly on individuals and induces indirect species and community level emergent properties from individual interactions. Because of our limited knowledge, any attempt to model the response of fish communities to environmental changes usually implies pragmatic compromises depending on the focal levels and scales of organization. For example, some approaches fully account for individual life history as well as intra- and inter-specific interactions on local scales with individuals based models (Grimm (1999) ; Shin & Cury (2001)), while others only model target species and their evolution in a changing environment (Lehodey et al. (2008) ; Dueri et al. (2014)). Yet other approaches focus on the species probability of occurrence as a func-

tion of given environmental variables with ecological niche models (Peterson (2003) ; Cheung et al. (2009)), others disregard species differences and only derive the ecosystem size-spectrum, namely the biomass distribution as a function of individuals' size (Maury et al. (2007) ; Blanchard et al. (2009, 2012) ; Woodworth-Jefcoats et al. (2013)).

Body size plays a dominant role in fish communities. It structures individual's life history and trophic interactions. Recent studies use both body size and the trait species maximum (or maturity) size as structuring variables to integrate through organization levels and account for the influence of functional biodiversity on community dynamics. These trait-based size-spectrum models link individual's bioenergetics to the specific structure to the emergent response of communities (Andersen & Beyer (2006) ; Hartvig et al. (2011) ; Maury & Poggiale (2013)). Similarly to physiologically structured populations models (Metz & Diekmann (1986) ; De Roos & Persson (2001, 2013)) these approaches account for environmental signals impacts across organization levels.

In this paper, we use a trait-based size-spectrum model presented in Maury & Poggiale (2013) to investigate the impact of the environment on fish communities. We focus on the impact of two major factors affected by climate change ; the lower trophic level biomass and water temperature. In the first section we summarize the model, especially how it links the individual's bioenergetics to the specific structure to community dynamics. The way environmental effects are introduced is also described. To analyze environmental impacts, indicators of the ecosystem state are derived. They characterize ecosystems in terms of structure, diversity and metabolism. The elicitation of the model's parameters is presented. In a second section we use this framework to analyze how the characteristics of fish communities are linked to the environment. The effects of lower trophic level biomass and temperature are first considered independently, before focusing on their combined impacts. Distinct trophic-length domains are observed over different lower trophic level biomass and temperature ranges. To bring realism into this idealized study, the structure of marine ecosystems is then investigated along a latitudinal gradient representative of mean tempera-

ture and mean lower trophic level biomass co-variations from South to North pole. Finally, the third section discusses the use of our mechanistic approach to explain features of global marine ecosystems. It agrees especially with the observation that larger species compose fish communities when latitude increases. The distinct trophic-length domains when changing lower trophic level biomass and temperature will lead to different sensitivities of fish communities to environment variations.

1. Method

1.1. Model

1.1.1. The trait-based community size-spectrum model

At the individual level, the model adopts a reduced formulation of the Dynamic Energy Budget theory (DEB, Kooijman (2000, 2010)) and represents the life history of fish individuals (Fig. 1). It dynamically prescribes the allocation of assimilated energy to growth in structural volume V (cm^3), respiration, maturation and reproduction during the life time of individuals. This life history is fully determined by : the quantity of food encountered which controls the satiation of individuals defined by a scaled Holling type II functional response (see $f_V^{V_m}$ section 1.1.2) ; the body temperature T (^oC), that increases or reduces metabolic rates (see T_{cor}, section 1.2.2). In the DEB theory, most processes scale with the maximum structural volume V_m that a species reaches in a favorable environment. Therefore, the theory represents the life history of individuals belonging to an infinite number of fish species with a same set of generic parameters (see DEB parameters Tab. 2 and section 1.4.2). It disregards other dimensions of species diversity since two individuals of different species with the same size V_m will be considered as functionally identical. But it models the main life history characteristics of the full range of fish species in an ecosystem keeping the model complexity tractable.

At species level, on a log-log scale the density of abundance $N_{V,t}^{V_m}$ (# cm^{-3} cm^{-3} m^{-3}) of fish individuals of a species of maximum size V_m can be represented as a function of their structural volume $V \in [V_b, V_m]$ with an abundance density spectrum (for V_b a birth volume). Each species characterized by $V_m \in [V_m^{min}, V_m^{max}]$, the range of specific traits of the community, can be represented with a distinct species spectrum (Fig. 1). These specific spectra are coupled to each other by predation. In aquatic ecosystems, predators are opportunists, their prey belong to any species and is calculated at spectra level using a size-selectivity predation function $s_{V_{Pr},V_{pr}}$ (between the predator V_{Pr} and prey V_{pr} structural volumes, see T4.f Appendix B). The abundance dis-

tribution and size-selectivity determine the predation mortality on preys and provides the prey biomass which controls predators' bioenergetics at individual level. Represented by the DEB for any predator of any species, this individual level bioenergetics in turn influences the dynamics of the species abundance distributions $N_{V,t}^{V_m}$. For instance, the DEB determines the energy (or biomass) allocated to reproduction, it is re-injected as eggs at a birth size V_b and relates to the intercept of the species abundance spectrum. The DEB determines the energy (or biomass) allocated to growth, it allows the species level advection of abundance through volumes V. Note that the effect of water temperature on individuals' metabolic rates similarly influences the dynamics of the species.

At the community level, the abundance density distribution $\mathrm{N}_{V,t}$ as a function of individuals' size $V \in [V_b, V_m^{max}]$ emerges as the integral of all species spectra on the size range $[V_m^{min}, V_m^{max}]$:

$$\mathrm{N}_{V,t} = \int_{V_m^{min}}^{V_m^{max}} N_{V,t}^{V_m} dV_m \ . \tag{1}$$

With the model, the individual bioenergetics influences the species' dynamics and explains the emergent fish community dynamics (Fig. 1). In detail, few additional processes complete the definition of the model. These include ageing and disease mortalities as well as schooling. See Maury & Poggiale (2013) for a detailed description of the model or Appendix A and B for the detailed summary of governing equations at individual and species/community levels. Note that the schooling (T4.g, Appendix B) is a process introduced to maintain coexistence of small and large fish species in the same community (Maury & Poggiale (2013)). It provides a threshold value below which preys are protected from predation and avoids the unrealistic depletion of smaller prey species by predation. This schooling also stabilizes communities avoiding spurious oscillations of the spectrum induced by predator-prey interactions.

This model allows the direct response of individuals bioenergetics to environmental perturbations and propagates the signal to species and community level abundance distributions. Because of the explicit representation of species

diversity, at the same size V individuals from different fish species of maximum size V_m have distinct life history properties. The same way at the same size a sardine and a yellowfin tuna do not have the same growth, mortality, food requirements, etc. These differences shape the food web properties and the sensitivity of ecosystems to their environment.

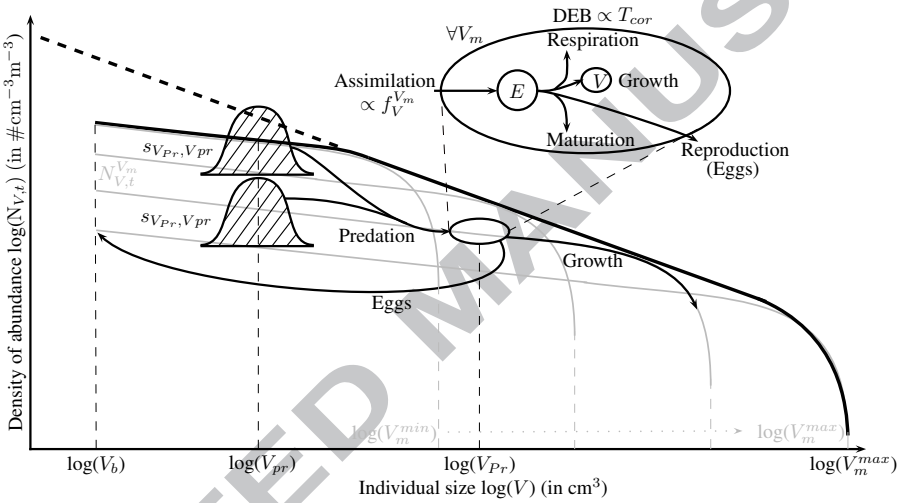

FIGURE 1 : Schematic representation of the fish community abundance density spectrum $N_{V,t}$ (black line) as a sum of species spectra $N_{V,t}^{V_m}$ (grey lines) emerging from the individual level DEB energy fluxes driven by size-selective predation (black arrows). Lower trophic level resource spectrum (dashed line).

1.1.2. The scaled functional response

The satiation of individuals controls the quantity of food they assimilate and indirectly affects their physiological performances, especially their growth or eggs production. For instance, at satiation an individual grows at maximum speed and produces maximum number of eggs, while in the opposite, when the

food is scarce the growth and the reproduction can be suspended, individuals may even die of starvation.

For an individual of size V and species maximum size V_m, this satiation is expressed with a Holling type II functional response (Holling (1959)) characterized by the capacity of the individual to : process food, limited by an handling time $h_V^{V_m}$; search and find food, limited by an attack rate $a_V^{V_m}$. Assuming the species' level energy (or biomass) density of prey p_V (see T4.h, Appendix B), this key component of the model writes :

$$f_V^{V_m} = \frac{p_V}{\frac{1.}{h_V^{V_m} a_V^{V_m}} + p_V} \ . \tag{2}$$

The handling time is directly linked to the maximum assimilation rate $\dot{p}_{Am_{max}}^{V_m}$ (see Appendix A) defined in the DEB theory as $\{\dot{p}_{Am}^{V_m}\}V^{2/3}$:

$$h_V^{V_m} = \frac{1.}{\dot{p}_{Am_{max}}^{V_m}} = \frac{1.}{\alpha_{\{\dot{p}_{Am}\}} V_m^{1/3} V^{2/3}} \ , \tag{3}$$

$\{\dot{p}_{Am}^{V_m}\} = \alpha_{\{\dot{p}_{Am}\}} V_m^{1/3}$ being the maximum surface-specific assimilation rate of an individual.

The attack rate is the product of individuals swimming speed, proportional to individuals length $L \propto V^{1/3}$, and the cross section of the capturing apparatus, proportional to $V^{2/3}$:

$$a_V^{V_m} = C V^{1/3} V^{2/3} = CV \ , \tag{4}$$

volume specific with C a dimensionless constant.

The functional response is a function of individuals' size V as well as species' maximum size V_m :

$$f_V^{V_m} = \frac{p_V}{\frac{\alpha_{\{\dot{p}_{Am}\}} V_m^{1/3} V^{2/3}}{CV} + p_V} = \frac{p_V}{C' V_m^{1/3} V^{-1/3} + p_V} \ , \tag{5}$$

for $C' \propto C^{-1} \alpha_{\{\dot{p}_{Am}\}}$ a semi-saturation constant. For the same prey density, the satiation of individuals depends on their size V but also on their species V_m. Different individuals of different species have different sensitivities to variations of their environment.

1.2. Environmental drivers

1.2.1. Lower trophic level biomass (LTL)

The lower trophic levels provide food to small fish individuals that are themselves eaten by larger individuals and so on. Perturbations of the lower trophic level biomass propagate up the trophic chain and alter the community properties. In the model, the lower trophic levels are represented using a constant slope log-log abundance density size-spectrum over the range $[V_{LTL}^{min}, V_{LTL}^{max}]$ (see Fig. 1). Small individuals fuel their bioenergetics feeding on this spectrum through size-selective predation (according to $s_{V_{Pr},V_{pr}}$, see T4.f Appendix B). In the present paper we focus on higher trophic levels properties. Therefore we disregard the effect of predation mortality exerted on this food resource and keep the lower trophic level total biomass ξ_{LTL} (expressed in term of energy in Jm^{-3}) constant during each simulation.

1.2.2. Temperature (T)

For most marine fish, water temperature has a direct influence on metabolic processes (Gillooly et al. (2001) ; Clarke & Fraser (2004)). The individual level DEB accounts for this influence with a correction of metabolic rates with temperature. This correction T_{cor} follows an Arrhenius relationship (see T4.r Appendix B, Kooijman (2000, 2010)), increasing or decreasing the metabolic rate for a temperature T compared to a reference metabolic value at reference temperature T_{ref}. Other metabolism's related processes such as feeding (see section 1.2.3), ageing and disease are also corrected with T_{cor}. All model parameters are determined at T_{ref} and the impact of temperature on fish communities is investigated simulating constant T levels (in ^oC) with a constant T_{cor} correction.

1.2.3. Temperature dependence of the scaled functional response

The processes related to food assimilation are temperature dependent : the maximum food assimilation $\dot{p}_{Am_{max}}^{V_m}$, the handling time $h_V^{V_m} = (\dot{p}_{Am_{max}}^{V_m})^{-1}$ and the attack rate $a_V^{V_m}$. When corrected with the Arrhenius relationship T_{cor} these processes scale differently with temperature (Englund et al. (2011) ; Rall et al.

(2012)), for instance T_{cor}^{-p} for handling time (or T_{cor}^{p} for maximum food assimilation) and T_{cor}^{q} for attack rate.

Including the temperature correction, the scaled functional response writes :

$$f_V^{V_m} = \frac{p_V}{\frac{\alpha_{\{\dot{p}_{Am}\}} V_m^{1/3} V^{2/3} T_{cor}^{p}}{C V T_{cor}^{q}} + p_V} = \frac{p_V}{C' V_m^{1/3} V^{-1/3} T_{cor}^{p-q} + p_V} \; ; \tag{6}$$

and the food assimilation (from T3.b, Appendix A) :

$$\dot{p}_A^{V_m} = f_V^{V_m} \dot{p}_{Am_{max}}^{V_m} T_{cor}^{p} \; . \tag{7}$$

Merging these two equations : at high food density, i.e. $p_V \gg C' V_m^{1/3} V^{-1/3} T_{cor}^{p-q}$, $f \approx 1$, the assimilation scales only with T_{cor}^{p} ; at low food density, i.e. $p_V \ll C' V_m^{1/3} V^{-1/3} T_{cor}^{p-q}$, the sensitivity to temperature of the scaled functional response matters, the assimilation scales with $T_{cor}^{-p+q} T_{cor}^{p} = T_{cor}^{q}$. It means that at high food density, the assimilation depends on the handling time which controls the temperature dependence. At low food density, the assimilation depends on the attack rate which controls the temperature dependence.

The selection of the scaling factors p and q in order to model fish communities is a challenge. For instance, Rall et al. (2012) estimated generic values in a meta-analysis (in term of activation energy), the scaling of attack rate appears higher than ingestion but smaller than metabolism (i.e. $p < q < 1$, since the metabolism scales with T_{cor}^{1}). Based on another meta-analysis, Englund et al. (2011) suggests the opposite relationship between attack rate and ingestion (i.e. $q < p < 1$). Here we choose a value of $p = 1$ to keep consistency within the DEB and $q = 1/3 < p$ from biomechanic considerations for the attack rate (i.e. $q < p = 1$).

1.3. Ecosystems indicators

1.3.1. Structure

We use a set of indicators to investigate quantitatively how lower trophic level biomass and water temperature impact the properties of ecosystems. Note that for the modeled ecosystems these indicators have constant values since the

model converges toward a stable steady state solution for every environmental forcing considered (see section 1.4.1).

On a log-log scale, the abundance community spectrum $N_{V,t}$ (Fig. 1) is known to display a quasi-linear shape that can be characterized by its slope S_C, and its intercept (Fulton et al. (2004) ; Shin et al. (2005)). This latter relates to the total abundance in the modeled community, or the total energy ξ_t^{tot} since abundance and energy contents are related in the model (see T4.d, Appendix B).

$$\xi_t^{tot} = \int_{V_m} \int_{V} \xi_{V,t}^{V_m} dV dV_m \ . \tag{8}$$

The abundance size distribution $N_{V,t}$ is also used to compute the cut-off size, the maximum structural size in the community. It is defined as the length L_{cut} ($\propto V_{cut}^{1/3}$) at which the abundance density ratio between two successive structural sizes class is less than 1/10 (Lefort et al. (2015)). We also compute trophic levels extracting $D_{V_{Pr},V_{pr}}$, the fraction of prey of size V_{pr} in the diet of predators of size V_{Pr} :

$$TL_{V_{Pr},t} = 1 + \sum_{V_{pr}} D_{V_{Pr},V_{pr}} TL_{V_{pr},t} \ . \tag{9}$$

Note that for simplicity the biomass at lower trophic levels is aggregated into a single reference lower trophic level. The trophic levels sustained in the fish community are computed from this reference.

We therefore use four indicators to characterize the fish community structure :

- ξ_t^{tot} (T1.a) : The total amount of energy (considered equivalent to biomass) in the modeled community (in Jm^{-3}).
- S_C (T1.b) : The community size-spectrum slope. It describes the relative abundance of small and large individuals in the community. It is usually assumed to be approximately constant with a value around -2 for an abundance density spectrum function of structural volumes V (Benoît & Rochet (2004) ; Andersen & Beyer (2006)).
- L_{cut} (T1.c) : The cut-off size. It is a simple indicator of the maximum length (in cm) of the species sustained in the community.

— $TL_{max,t}$ (T1.d) : The trophic level $TL_{V_{Pr},t}$ of individuals in the larger size class sustained in the community. It characterizes the trophic chain length.

Figure 2 represents schematically some of these indicators while all are detailed in the table 1.

1.3.2. Diversity

While the size distribution characterizes the structure, the distribution of species maximum sizes characterizes the diversity in the community. Every specific spectrum $N_{V,t}^{V_m}$ in the range $[V_m^{min}, V_m^{max}]$ contributes to the fish community size-spectrum $\mathrm{N}_{V,t}$. This contribution can be described at every individuals structural size by the $\Phi_{V,t}^{V_m}$ function (Maury & Poggiale (2013)) :

$$N_{V,t}^{V_m} = \Phi_{V,t}^{V_m} \mathrm{N}_{V,t} \qquad \text{and} \qquad \int_{V_m^{min}}^{V_m^{max}} \Phi_{V,t}^{V_m} dV_m = 1 \ . \tag{10}$$

We compute an indicator of diversity based on $\Phi_{V,t}^{V_m}$ and a « map » of species maximum size diversity in modeled communities (Fig. 2). The « map » represents the maximum length $L_m \propto V_m^{1/3}$ at the 5^{th} ($L_m(\Phi_{V,t}^{5\%})$), 50^{th} ($L_m(\Phi_{V,t}^{50\%})$) and 95^{th} ($L_m(\Phi_{V,t}^{95\%})$) percentiles of the $\Phi_{V,t}^{V_m}$ distribution as a function of individuals' length $L \propto V^{1/3}$. It represents the diversity of lengths of species carrying the biomass flow at different individuals' sizes.

We therefore use two indicators of the fish community diversity (see Fig. 2 and Tab. 1) :

— $\overline{\overline{L}}_m$ (T1.e) : The geometric mean of species maximum lengths (in cm). It determines the kind of species contributing to the community, small or large.

— $\overline{\Delta L}_m$ (T1.f) : The species maximum size variability (in cm). It is the mean value of the maximum sizes spread $\overline{(L_m(\Phi_{V,t}^{95\%}) - L_m(\Phi_{V,t}^{5\%}))}$ over the diversity « map ». It describes the functional diversity of biomass pathways. When it is small, the biomass flow in the community is carried by species of similar maximum sizes. When it is large, a wide range of

alternative biomass pathways are provided by species of very different sizes.

Note that different species spectra provide different biomass pathways from small to large individuals, but they provide no measure of the number of species in the community. Indeed, one species spectrum characterized by a maximum size $V_m \in [V_m^{min}, V_m^{max}]$ represents one as well as ten species characterized by a maximum size V_m. The model represents the role of species functional diversity but provides no measure of species richness.

1.3.3. Metabolism

The model links the metabolism of individuals to the community. At the individual level, the DEB theory explicitly prescribes the allocation of ingested biomass into reserve or structure (see DEB representation, Appendix A). The model explicitly computes attributes of metabolism :

— consumption $\dot{p}_X^{V_m} = \dot{p}_{X,LTL}^{V_m} + \dot{p}_{X,C}^{V_m}$ (T3.a, Appendix A) by predators of species V_m, where $\dot{p}_{X,LTL}^{V_m}$ is the biomass (or energy) ingested from the lower trophic level biomass pool and $\dot{p}_{X,C}^{V_m}$ is ingested from other fish in the community.

— production $\dot{p}_E^{V_m} + \dot{p}_G^{V_m}$ (T3.d,f Appendix A) by individuals of species V_m by transformation of ingested energy into organic matter in reserves or structure.

Knowing the abundance distribution $N_{V,t}^{V_m}$, the community level consumption of lower trophic level biomass, $\dot{P}_{LTL,t}$, and production $\dot{P}_{Prod,t}$ are :

$$\dot{P}_{LTL,t} = \int_{V_m} \int_{V} \dot{p}_{X,LTL}^{V_m} N_{V,t}^{V_m} dV dV_m \ , \dot{P}_{Prod,t} = \int_{V_m} \int_{V} \left(\dot{p}_E^{V_m} + \dot{p}_G^{V_m} \right) N_{V,t}^{V_m} dV dV_m. \tag{11}$$

We therefore use two indicators to characterize the metabolism at the community level :

— $R^{Prod} = \dot{P}_{Prod,t} / \dot{P}_{LTL,t}$ (T1.g) : The efficiency of the community to transform the resource preyed on lower trophic levels into fish biomass.

— $t_{res} = \xi_t^{tot}/\dot{P}_{LTL,t}$ (T1.h) : At steady state, the biomass preyed on the lower trophic level biomass balances dissipation and losses (Appendix D). This biomass consumed characterizes the residence time, the mean time spent by biomass in the community (in d). It is an indication of the speed of the biomass flow in the community.

Table 1 summarizes all the fish community indicators of structure, diversity and metabolism.

TABLE 1 : Summary of model's indicators for stucture, diversity and metabolism. These are constant values for every environmental forcing considered.

Eq.	Indicator	Equation
Structure		
T1.a	Total energy/biomass	$\xi_t^{tot} = \int_{V_m}\int_{V} \xi_{V,t}^{V_m} dV dV_m$
T1.b	Spectrum slope	S_C
T1.c	Cut-off size	$L_{cut} \propto V_{cut}^{1/3}$ the length class where $\mathrm{N}_{V_{cut},t} < 10\ \mathrm{N}_{V_{cut}-\Delta V,t}$
T1.d	Maximum trophic level	$TL_{max} = max(TL_{V_{Pr},t})$ with $TL_{V_{Pr},t} = 1 + \sum_{V_{pr}} D_{V_{Pr},V_{pr}} TL_{V_{Pr},t}$
Diversity		
T1.e	Mean species maximum size	$\overline{L}_m = exp\left(\frac{\int_{L_m}\int_{L} ln(L_m) N_{L,t}^{L_m} dL dL_m}{\int_{L_m}\int_{L} N_{L,t}^{L_m} dL dL_m}\right)$ with $L_m = \frac{V_m^{1/3}}{\delta}$
T1.f	Variability of species maximum size	$\overline{\Delta L}_m = \frac{\int_{L_m}\int_{L} (L_m(\Phi_{t,L}^{95\%}) - L_m(\Phi_{t,L}^{5\%})) dL dL_m}{\int_{L_m}\int_{L} dL dL_m}$ with $L_m = \frac{V_m^{1/3}}{\delta}$
Metabolism		
T1.g	Production efficiency	$R^{Prod} = \frac{\dot{P}_{Prod,t}}{\dot{P}_{LTL,t}} = \frac{\int_{V_m}\int_{V} \dot{p}_E^{V_m} + \dot{p}_G^{V_m}\ \ N_{V,t}^{V_m} dV dV_m}{\int_{V_m}\int_{V} \dot{p}_{X,LTL}^{V_m} N_{V,t}^{V_m} dV dV_m}$
T1.h	Residence time	$t_{res} = \frac{\xi_t^{tot}}{\dot{P}_{LTL,t}} = \frac{\int_{V_m}\int_{V} \xi_{V,t}^{V_m} dV dV_m}{\int_{V_m}\int_{V} \dot{p}_{X,LTL}^{V_m} N_{V,t}^{V_m} dV dV_m}$

1.4. Simulations

1.4.1. Numerical setting

Indicators are compared to solutions of the model at different constant lower trophic level biomass and water temperatures. The system of governing equations (see table 4, Appendix B) is solved for a set of species spectra using an explicit donor-cell finite volume algorithm on a discretization of 100 structural volumes to approximate the advection term (T4.a). The discretization

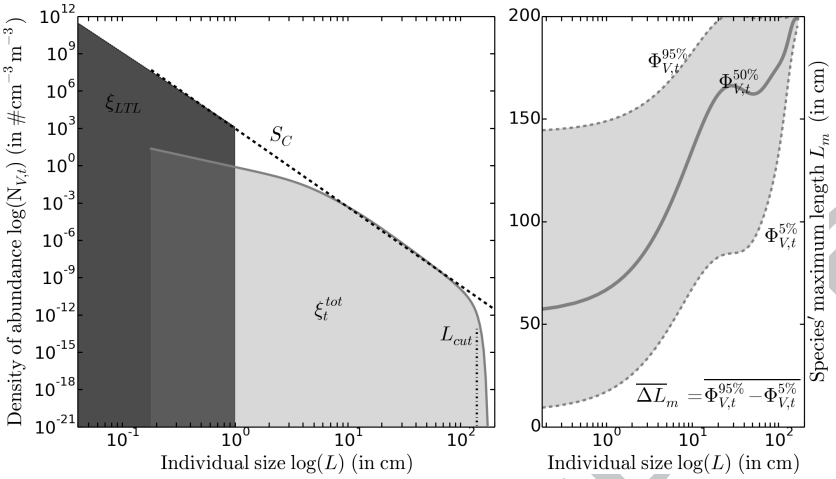

FIGURE 2 : Schematic representation of indicators : left, lower trophic level abundance density size-spectrum (black), community abundance density size-spectrum (grey) and indicators, slope S_C, cut-off size L_{cut} (in cm) and total energy $\xi_L TL/\xi_t^{tot}$ (in Jm^{-3}) ; right, diversity map (grey) and species maximum size variability $\overline{\Delta L}_m$ (in cm).

is non uniform, with increasing resolution toward the smallest size classes for computational performances. It ranges from $L_b = 0.1\ cm$ ($\propto V_b^{1/3}$) for eggs to $L_m^{max} = 200\ cm$ ($\propto V_m^{max\ 1/3}$). An irregular discretization of 77 species maximum sizes L_m is chosen on the same size range. The numerical simulations run with a daily time step and start from an arbitrary residual initial state. They run until the system reaches a stable steady solution, after few simulated decades for the fast living communities, or few simulated centuries for the slow living communities.

Representative ranges for lower trophic level biomass ξ_{LTL} and temperature T are inferred from a climatological simulation of the coupled NEMO-PISCES physics-biogeochemistry model (Aumont et al. (2015)). For that purpose, phytoplankton and zooplankton biomass concentration on a 1° grid are converted into energy content distributions. Pulled together they are associated to a size range $[L_{LTL}^{min}, L_{LTL}^{max}] = [0.001\ cm, 1\ cm]$ and averaged over longitudes to provide mean latitudinal distributions of lower trophic level biomass. From these we keep the annual mean and variability represented by the 5^{th} and 95^{th} percen-

tiles (Fig. 3). Similarly, temperature values have been derived from the spatial and time distributions of sea surface temperatures in the NEMO-PISCES model, averaged in longitude, keeping annual mean and variability between the 5^{th} and 95^{th} percentiles of the latitudinal distributions (Fig. 3).

1.4.2. Parameters

At the individual level, the DEB parameters (Tab. 2) are adapted from the generic ones (Kooijman (2010)) to better account for fish communities (Appendix D and Kooijman & Lika (2014)). Note that the temperature correction of these DEB parameters is based on an Arrhenius temperature of $8000°K$ consistent with a mean value $Q_{10} = 2.36$ of the van't Hoff coefficient for species of teleost fishes compiled in Clarke & Johnston (1999). However, this correction only increases or decreases the metabolism of individuals around a resting metabolic rate while on large scale this resting metabolic rate also depends on an Arrhenius temperature correction. Since our analysis focuses on large scale environmental effects, especially across latitudes, we modified the Arrhenius temperature in order to represent this large scale effect. According to the evolutionary trade-off hypothesis, an Arrhenius temperature $T_A = 5370°K$ ($Q_{10} = 1.83$) is selected to correct the resting metabolism of individuals (Clarke & Fraser (2004)).

At the species level, the size-selective predation is the main constraint on biomass transfer between size class. It is parameterized so that the modeled distribution of prey size L_{pr} ($\propto V_{pr}^{1/3}$) in the stomach of predators of size L_{Pr} ($\propto V_{Pr}^{1/3}$) matches empirical observations taken from Scharf et al. (2000). These observations are based on a long-term collection of prey size distribution in the stomach of 18 predator fish species on the continental shelf along the northeast US coast. The parameters of the model α_1, α_2, γ_1 and γ_2 of the size-selectivity function $s_{V_{Pr},V_{pr}}$ (see T4.f Appendix B) are tuned so that the mean, 5^{th} and 95^{th} percentiles of the modeled prey distributions in predators stomach match the mean, 5^{th} and 95^{th} percentiles of the prey distributions derived from data (Fig. 4).

Four last parameters are free in the model, they control (see Appendix B) : the disease mortality (D, T4.n), the ageing ($\ddot{h}_a$, T4.o), the schooling (s_{cr}, T4.g) and the functional response (C', T4.k). While the parameterization of the disease mortality and schooling defines the fish community intercept, the ageing and half saturation constant C' tune the extent of the spectrum. These parameters are determined over the wider range of lower trophic level biomass $\xi_{LTL} \in [50\ Jm^{-3}, 8000\ Jm^{-3}]$ at an associated environmental temperature $T = 5°C$ (see Fig. 3). The criteria for their determination are that, with a single set $(D, \ddot{h}_a, C', s_{cr})$: at the lowest level 50 Jm^{-3}, the community spectrum characterizes a poor ecosystem, with few species spectra sustained ; at the highest level 8000 Jm^{-3}, the community spectrum is completely developed, with all species spectra sustained ; at intermediate level 1200 Jm^{-3}, the community spectrum is partially developed. In addition, according to the spectrum theory the biomass distribution in logarithmically equal particles size pools from $\ll$ plankton to whales $\gg$ is constant (Sheldon et al. (1972)). It implies the alignment of fish community and lower trophic level size-spectra. This last criteria is enforced at intermediate level 1200 Jm^{-3} with the same set $(D, \ddot{h}_a, C', s_{cr})$. Figure 5 illustrates the obtained spectra. Such parameterization allows large variations of the fish community features on the selected range of environmental conditions.

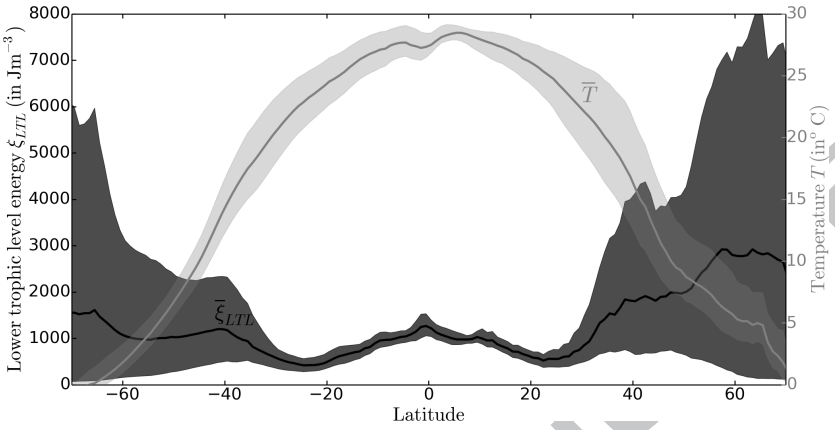

FIGURE 3 : Latitudinal distribution of the environmental conditions determined from NEMO-PISCES outputs (Aumont et al. (2015)) and used to force the model : annual mean $\overline{\xi}_{LTL}$ (in Jm^{-3}) and monthly variability of lower trophic level energy ξ_{LTL} (black) ; annual mean $\overline{T}$ (in $°C$) and monthly variability of sea surface temperature T (grey).

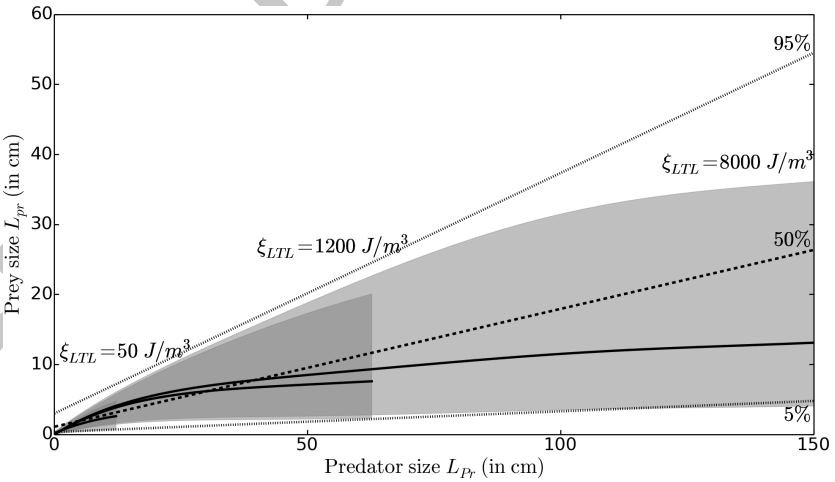

FIGURE 4 : Prey size distribution in the stomach of predators : as derived from empirical data detailed in Scharf et al. (2000) (·· percentiles and –– mean) ; as modeled at various lower trophic level energy $\xi_{LTL} = 50,\ 1200,\ 8000\ Jm^{-3}$ at $T = 5°C$ (grey domains with ▬ mean).

TABLE 2 : Summary of models parameters used for numerical simulation, values and references.

Variable	Designation	Unit	Value	Ref
Individual's DEB				
E / E^*	Energy of the reserve/ at equilibrium	J	–	Maury & Poggiale (2013)
V / L	Structural volume/length	cm^3/cm	$\begin{cases} V = (\delta L)^3 \\ \delta = 0.2466 \end{cases}$	Maury & Poggiale (2013)
V_m / L_m	Species maximum structural volume/length	cm^3/cm	$V_m = (\delta L_m)^3$	Kooijman (2010)
V_p	Puberty structural volume	cm^3	$\begin{cases} V_p = \alpha_p V_m \\ \alpha_p = 0.125 \end{cases}$	Kooijman & Lika (2014)
$\{\dot{p}_{A_m}^{V_m}\}$	Maximum surface-specific assimilation rate	$J\ cm^{-2} d^{-1}$	$\begin{cases} \alpha_{\{\dot{p}_{Am}\}} V_m^{1/3} \\ \alpha_{\{\dot{p}_{Am}\}} = 31.25 \end{cases}$	Appendix D
$[E_m^{V_m}]$	Maximum reserve density	$J\ cm^{-3}$	$\begin{cases} \alpha_{[E_m]} V_m^{1/3} \\ \alpha_{[E_m]} = 312.5 \end{cases}$	Appendix D
ν	Energy conductance $\{\dot{p}_{A_m}^{V_m}\}/[E_m^{V_m}]$	$cm\ d^{-1}$	0.1	Appendix D
$[\dot{p}_M]$	Maintenance rate	$J\ m^{-3} d^{-1}$	25.	Kooijman & Lika (2014)
$[E_G]$	Volume specific cost of growth	$J\ cm^{-3}$	5691.	Appendix D
κ_X	Assimilation efficiency	–	0.8	Maury & Poggiale (2013)
κ	Energy fraction allocated to growth and maintenance	–	0.8	Maury & Poggiale (2013)
κ_R	Energy fraction of gonads turned into eggs	–	0.95	Kooijman (2010)
$\ddot{h}_a$	Ageing acceleration	d^{-2}	45. 10^{-8}	Section 1.4.2
Community's biology				
C'	Half saturation constant of the functional response	$J\ d^{-1}$	3.5	Section 1.4.2
D	Maximum mortality rate due to disease	d^{-1}	0.4	Section 1.4.2
M_{egg}	Fraction of spawned eggs not fertilized	–	0.8	–
φ	Sex-ratio (Mean proportion of female)	–	0.5	–
d	Density of biomass	$g\ cm^{-3}$	1.	–
ψ	Energy content of biomass	$J\ g^{-1}$	4552.	Appendix D
Predation				
(ρ_1, ρ_2)	Mean mini/maxi ratio predator over prey lengths	–	(2.5, 10.)	Section 1.4.2
(α_1, α_2)	Variability mini/maxi ratio predator over prey lengths	–	(5., 0.08)	Section 1.4.2
Schooling				
β	Shape of the schooling probability function	–	2.	Section 1.4.2
s_{cr}	Schooling probability threshold	m^{-6}	0.005	Section 1.4.2
Environment				
ξ_{LTL}	Lower trophic level biomass/energy	$J\ m^{-3}$	–	Section 1.4.1
T	Temperature	$°K/°C$	$°K =° C + 273.15$	–
T_A	Mean Arrhenius temperature	$°K$	5370.	Section 1.4.2
T_{ref}	Reference temperature of biological parameters	$°K$	293.15	Section 1.4.2
$-p$	Scaling exponent of the handling time	–	1	Section 1.2.3
q	Scaling exponent of the attack rate	–	1/3	Section 1.2.3
Numerical parameters				
$[L_b, L_m^{max}]$	Consumers' spectrum size range	cm	$[0.1, 200.]$	Section 1.4.1
$[L_{LTL}^{min}, L_{LTL}^{max}]$	Lower trophic level spectrum size range	cm	$[0.001, 1.]$	Section 1.4.1
Δt	Time step	d	1	Section 1.4.1

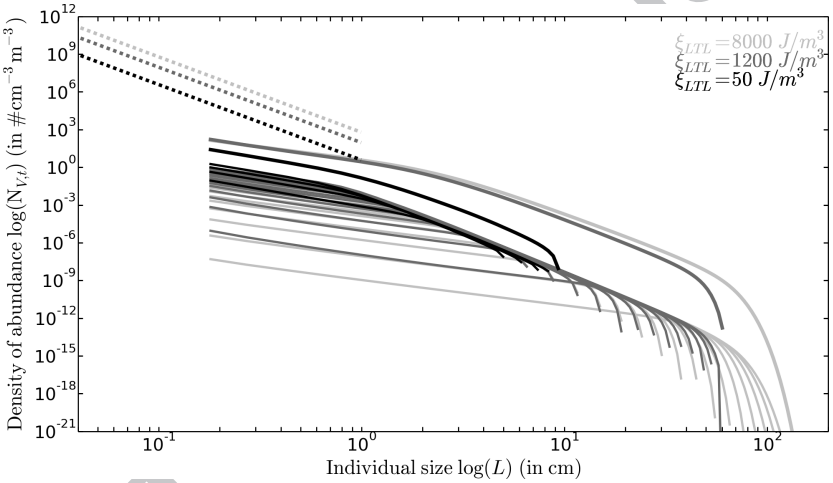

FIGURE 5 : Lower trophic level (dashed lines), community (thick line) and species (thin lines) size-spectra function of individual sizes L (in cm, $\propto V^{1/3}$) at different lower trophic level energy $\xi_{LTL} = 50,\ 1200,\ 8000\ Jm^{-3}$ and at $T = 5°C$ for a single set $(D, \ddot{h}_a, C', s_{cr})$.

2. Results

2.1. Separate lower trophic level biomass and water temperature impact

2.1.1. A multi-domain response

The effects of lower trophic level biomass on fish communities are first observed over the range $\xi_{LTL} \in [50\ Jm^{-3}, 8000\ Jm^{-3}]$ keeping the temperature constant $T = 5°C$. The effects of temperature are observed over the range $T \in [0°C, 30°C]$ keeping the lower trophic level biomass constant $\xi_{LTL} = 3000\ Jm^{-3}$ (based on Fig. 3). Both sets of experiments reveal similar community level responses (Fig. 6), with four distinct trophic-length domains of community properties for distinct trophic chain length (TL_{max}).

Minimum ($\mathbf{TL_{max} \simeq 2}$*)*

A minimum trophic-length domain characterized by a minimal total community biomass (ξ_t^{tot}) at low resource (ξ_{LTL}), or high temperature (T). In this domain, communities are constituted of small individuals (L_{cut}) of primary consumers ($TL_{max} \simeq 2$) exclusively feeding on the lower trophic level spectrum.

Within the minimum trophic-length domain, increasing resource (ξ_{LTL}) or decreasing temperature (T) leads to a slow increase of the maximum size of individuals (L_{cut} increases) and the development of larger species ($\overline{\overline{L}}_m$ increases), without interactions within and between them since individuals exclusively feed on the resource ($TL_{max} \simeq 2$). There is no intra-community predation. While larger species develop, small individuals become dominant since every species has individuals in small size class, but only larger species bring individuals in larger size class (S_C decreases). The variability of species maximum sizes ($\overline{\Delta L}_m$) is minimum because of a reduced range of species supported.

Note that the minimum trophic-length domain is not visible over the range of temperatures explored figure 6. It appears at very low food level ξ_{LTL} (see distributions Fig. 7b at $\xi_{LTL} = 200\ Jm^{-3}$).

Low ($\mathbf{2 < TL_{max} < 2.5}$*)*

Within the low trophic-length domain, the variation of fish production (R^{Prod}) is attenuated compared to the minimum domain. Communities also include pri-

mary consumers, but with larger individuals (L_{cut}) and larger species ($\overline{\overline{L}}_m$) preying up to half of their diet on fish ($2 < TL_{max} < 2.5$).

With larger individuals in the community, intra-community predation starts exerting a top-down pressure on small size classes. The relative abundance of small and large individuals remains seemingly constant (small S_C variation) when environmental conditions vary. This is a consequence of the intra-community predation which harvests preferentially the most abundant small species that are forming schools, to the benefit of larger species. In the low trophic-length domain, the total fish biomass (ξ_t^{tot}) is less sensitive to variations than in the minimum trophic-length domain.

Medium ($\mathbf{2.5 < TL_{max} < 3}$*)*

Increasing lower trophic level biomass (ξ_{LTL}) or decreasing temperature (T) within the medium trophic-length domain leads to greater variations of the total community biomass (ξ_t^{tot}) than within the low domain. Very large individuals can be supported (L_{cut} increases). Secondary consumers develop for which more than half of the diet comes from fish consumers ($2.5 < TL_{max}$).

In this regime, individuals from large species feed on resource at lower trophic level when they are small and mainly on the fish community when they grow bigger. With this ontogenetic diet shift and apparition of secondary consumer the fish community is now providing food for its own development, enhancing the predation pressure on smaller size class. The schooling ensures the coexistence between large and small species and avoids the unrealistic complete depletion of small species. Therefore, with lower trophic level biomass or temperature variations, the relative abundance of large against small species fixed by schooling changes (S_C increases, decreases). Moreover, the species maximum size variability is enhanced ($\overline{\Delta L}_m$ increases), the food web includes more functional species from small to large. With secondary consumers in the community the energy derived from the resource is used for the development of more than one individual. Compared to the previous domains it enhances the community development, the size of the largest individuals (L_{cut}) increases sharply and the

efficiency to transform resource into biomass (R^{Prod}) is enhanced.

High ($\mathbf{TL_{max} \simeq 3}$*)*

Within the high trophic-length domain, communities reach their maximum biomass level (ξ_t^{tot}). Fish production (R^{Prod}) becomes independent of resource (ξ_{LTL}) or temperature (T) variations. A tri-trophic system of primary producers, primary consumers and secondary consumers is established ($TL_{max} \simeq 3$).

The community size-spectrum is fully developed and the functional response reaches saturation for all individuals of all species. An optimal balance between bottom-up energy supply, top-down predation pressure, energy dissipation and losses maintains the full community. The length of the largest individuals (L_{cut}) as well as the mean species size ($\overline{\overline{L}}_m$) reach their maximum. Coexistence allows the presence of a large range of species spectra, the species maximum size variability ($\overline{\Delta L}_m$) is maximum. Some indicators are not completely fixed however and reveal a slight structural reorganization of the community, such as variations of the relative abundance of small and large individuals (S_C). At a given food density or temperature, smaller species are closer to satiation ($f_V^{Vm} \propto V_m^{-1/3}$, section 1.1.2). When resource increases or temperature decreases, the largest species are the last to reach saturation. They slowly increase their dominance over the community and slowly modify its structure.

Note that the high trophic-length domain is not fully visible over the range of temperatures explored figure 6. It appears more clearly at very high food levels ξ_{LTL} (see distributions Fig. 7b at $\xi_{LTL} = 8000\ Jm^{-3}$).

2.1.2. Impact of lower trophic level biomass

The community develops non linearly when the lower trophic level biomass increases (Fig. 6 left). The biomass increase (ξ_t^{tot}) is faster than the lower trophic level biomass increase in the minimum trophic-length domain, tends to become proportional ($\propto \xi_{LTL}^{+1}$) in the low trophic-length domain and is faster again in the medium trophic-length domain before reaching a plateau ($\propto \xi_{LTL}^{0}$) in the high trophic-length domain.

In the framework of the DEB theory, the individual costs of maintenance are constant at individual level at a given structural volume V (T1.e,g and reproduction overhead, Appendix A). An increase in food availability (ξ_{LTL}) thus releases more energy for growth. It allows species to develop larger individuals (L_{cut} increases) and communities to sustain larger species ($\overline{\overline{L}}_m$ increases). The associated variability of species maximum length increases ($\overline{\Delta L}_m$). The tri-trophic structure explains the non linear relationship between resource and consumers biomass.

The residence time of energy derived from the lower trophic level also follows this multi-domain dependence. At a given size and scaled functional response, individuals of larger species grow faster. With increasing lower trophic level biomass, larger species are sustained, the flow of biomass is enhanced, and the residence time (t_{res}) globally decreases.

In the meantime, with the increase of the community size span (L_{cut}) and the elongation of the trophic chain (TL_{max}) a unit of biomass preyed on the resource supports more and more trophic levels. It induces an implicit increase of the residence time which mitigates the global decrease of the residence time (t_{res}) and explains its different slopes in each domain. Note that in the medium trophic-length domain this increase actually dominates the global enhancement of the biomass flow, t_{res} increases before decreasing again.

2.1.3. Impact of temperature

The community shrinks non linearly when the temperature increases (Fig. 6 right). Warming mostly enhances the speed of the biomass flow through the community (t_{res} continuously decreases). But because of different sensitivities to temperature of assimilation (scaling between T_{cor}^q ($q = 1/3$) and T_{cor}^p ($p = 1$)) and metabolism ($\propto T_{cor}$, see DEB Appendix A) the community shrinks.

At equilibrium, the community can be looked at as an open system with the food ingested from the resource strictly balanced by the community level losses and dissipation (Appendix C). At cold temperature, all individuals in a community access enough food to be at satiation, assimilation depends on T_{cor}^p ($p = 1$).

The metabolism, and as a matter of fact the loss and dissipation, also scales with T_{cor}. The variations of ingestion on the lower trophic level induced by the temperature are balanced by the same variations of losses and dissipation. The community is globally unaffected by temperature. Therefore, at colder temperatures in the high trophic-length domain the total fish biomass ξ_t^{tot} is invariant to temperature variations ($\propto T_{cor}^0$). Under warming conditions, the assimilation (between T_{cor}^q and T_{cor}^p) increases slower than the loss and dissipation ($\propto T_{cor}$). The energy entering the community becomes smaller or equal to the dissipation and loss. The community loses energy, the total biomass decreases with warming in the medium and low trophic-length domains. Ultimately, all individuals become food limited. The ingestion is limited by the attack rate which scales with T_{cor}^q and the metabolism scales with T_{cor} so that the fish total biomass decreases proportionally to $T_{cor}^{(q-1)}$ in warm ecosystems.

In this community level decrease of the total biomass with warming, the largest individuals disappear first because of a higher metabolic demand, the maximum individuals size (L_{cut}), mean species size ($\overline{\overline{L}}_m$) and species size variability ($\overline{\Delta L}_m$) decrease with warming.

2.2. Combined lower trophic level biomass and water temperature impact

2.2.1. Phase diagram

The separate effects of lower trophic level biomass and temperature over the ranges $\xi_{LTL} \in [50\ Jm^{-3}, 8000\ Jm^{-3}]$ and $T \in [0°C, 30°C]$ are now investigated at respectively distinct constant temperatures T and distinct constant biomass ξ_{LTL}. The multi-domain response is maintained but is shifted and attenuated (Fig. 7).

At various constant temperatures, the trophic-length domains succession when at various resource levels is modified (Fig. 7a) : in cold waters, the domains transitions occur earlier in these more productive communities ; in warmer waters, the domains cover wider resource ranges in these less productive communities. It implies that cold waters communities sustain larger individuals at lower food levels than they would in warm waters. At different food levels the

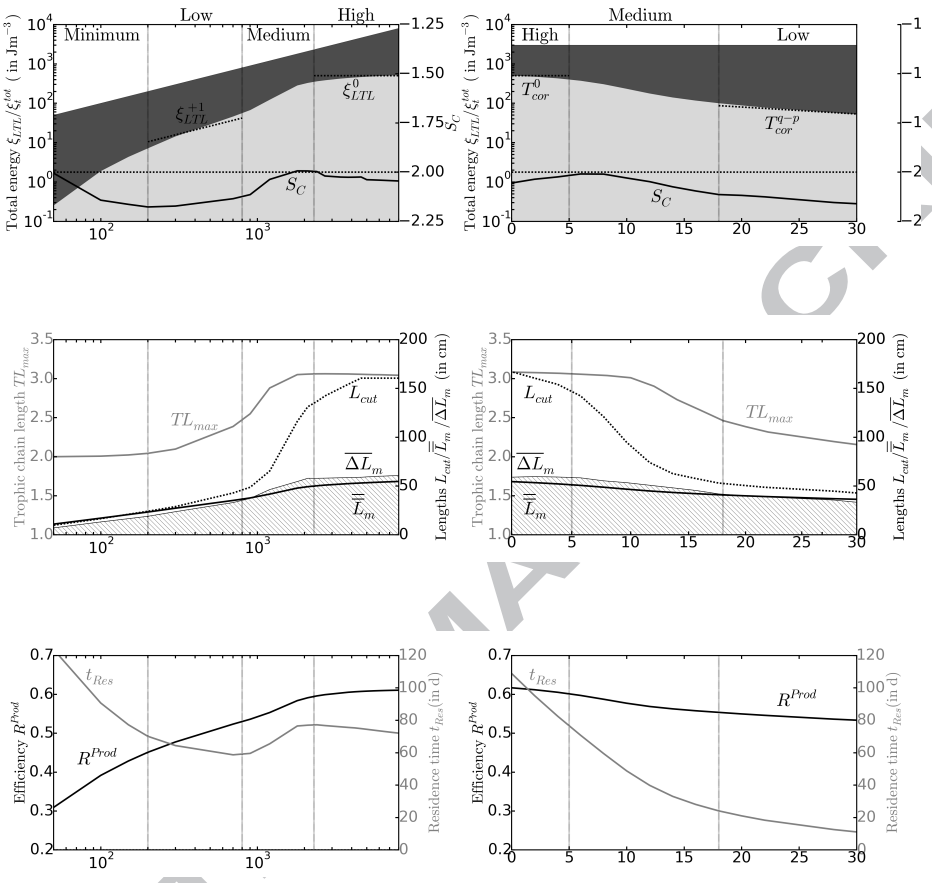

FIGURE 6 : Multi-domain responses of the community level indicators, left lower trophic level biomass $\xi_{LTL} \in [50\ Jm^{-3}, 8000\ Jm^{-3}]$ impact, right temperature $T \in [0°C, 30°C]$ impact, from top to bottom : total energy of the lower trophic level ξ_{LTL} (black) and community ξ^{tot}_t (grey, in Jm^{-3}), community slope S_C (black line) ; middle, maximum trophic level TL_{max} (grey line), cut-off size L_{cut} (dashed line, in cm), mean species lengths $\overline{\overline{L}}_m$ (black line, in cm) and species maximum size variability $\overline{\Delta L}_m$ (hatched, in cm) ; bottom, biomass production efficiency R^{Prod} (black line), residence time t_{Res} (grey line, in d).

domains succession with temperature has similar characteristics (Fig. 7b). Oligotrophic ecosystems display an earlier community shrinking and have sharper domains transitions.

Figure 7c summarizes the combined influences of resource and temperature

with a phase diagram. It represents the different trophic-length domains transitions and the different widths of these domains as a function of lower trophic level biomass (ξ_{LTL}) and temperature (T). As described in section 2.1.1, different domains are dominated by primary or secondary consumers and have different properties. On this figure, the mean environmental conditions $[\overline{\xi}_{LTL}, \overline{T}]$ along the latitudinal gradient figure 3 are superimposed. Different latitudes of the northern and southern hemisphere fall into different trophic-length domains and thus exhibit different properties. A global temperature increase of 2^oC on the mean environmental conditions shifts the latitudinal section in the phase diagram.

Note that the definition of the four free parameters (see section 1.4.2) actually places given environmental conditions in the phase diagram, but the trophic-length domains succession is conserved. In other words, another choice for the set $(D, \ddot{h}_a, C', s_{cr})$ would shift the domains succession in the phase diagram, for example towards higher resource levels or lower temperatures. It may also either expand or shrink the different domains. Our choice of parameters allows a succession of domains along the latitudinal section and reproduces an increase of mean species length with latitudes (see section 2.2.2).

2.2.2. Latitudinal gradient

To bring realism into our idealized study, the combined effect of lower trophic level biomass and temperature is simulated along the mean latitudinal gradient $[\overline{\xi}_{LTL}, \overline{T}]$ (see Fig. 3). Figure 8 illustrates the obtained indicators.

From low to mid-latitudes, the total biomass (ξ_t^{tot}) follows the resource (ξ_{LTL}). Communities are dominated by small and medium species of primary consumers ($TL_{max} \approx 2$). Moving towards higher latitudes, colder temperatures reduce maintenance costs and allow the development of larger individuals (L_{cut} increases) as well as larger species ($\overline{\overline{L}}_m$ increases). It enhances the fish biomass supported and indicators change like in the medium trophic-length domain defined previously. Secondary consumers develop, the trophic chain length (TL_{max}) and slope (S_C) increase. Finally, abundant food-saturated species become do-

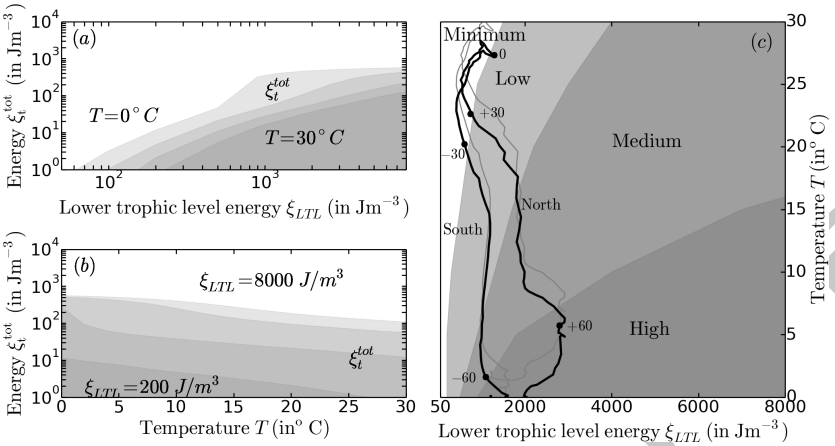

FIGURE 7 : Combined impact of lower trophic level biomass and water temperature : (a) total energy in the community ξ_t^{tot} (in Jm^{-3}) over the resource range $\xi_{LTL} \in [50\ Jm^{-3}, 8000\ Jm^{-3}]$ at various constant temperature levels $T \in [0°, 30°]$; (b) total energy in the community ξ_t^{tot} (in Jm^{-3}) over the temperature range $T \in [0°, 30°]$ at various constant lower trophic level energy $\xi_{LTL} \in [200\ Jm^{-3}, 8000\ Jm^{-3}]$; (c) phase diagram of the four trophic-length domains at distinct environmental conditions with mean environmental conditions along the latitudinal gradient, as derived from NEMO-PISCES (Fig. 3, black line) and shifted according to a global temperature increase of 2^oC (grey line).

minant at high latitude.

From the equator to the poles, modeled communities transform from dominated by small (small $\overline{\overline{L}}_m$), fast living (small t_{res}) species to dominated by large (large $\overline{\overline{L}}_m$) slow living (large t_{res}) species. When larger species are sustained, more species coexist because of schooling, the variability of species maximum length increases up to a plateau at higher latitudes ($\overline{\Delta L}_m$). Interestingly, the simulated values for the increase with latitude in geometric mean species length ($\overline{\overline{L}}_m$) respects the range of values empirically measured and detailed in Fisher et al. (2010). These data represent the geometric mean species length in large marine ecosystems (LME) at latitudes derived from approximate midpoints per LME.

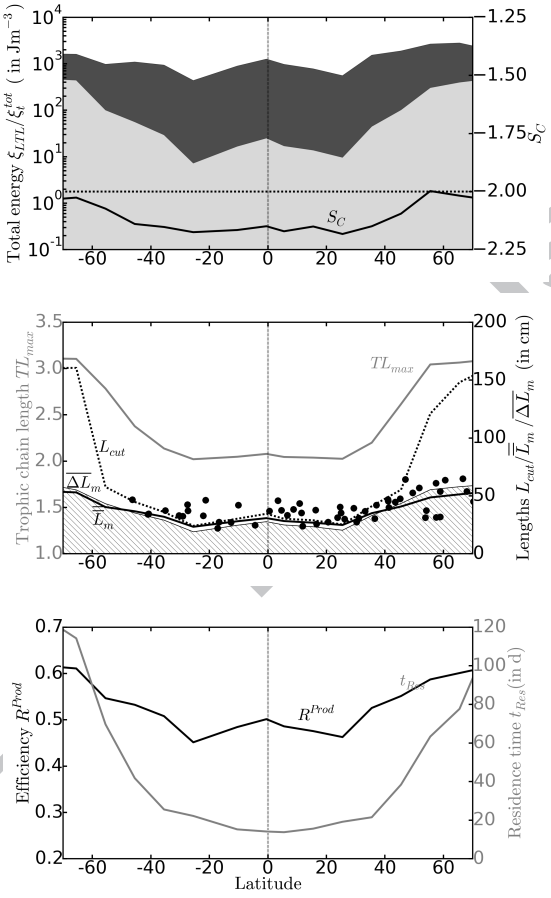

FIGURE 8 : Variations of the community level indicators along a latitudinal gradient of mean environmental conditions $[\overline{\xi}_{LTL}, \overline{T}]$ derived from outputs of the NEMO-PISCES model. From top to bottom : total energy of the lower trophic level ξ_{LTL} (black) and community ξ_t^{tot} (grey, in Jm^{-3}), community slope S_C (black line) ; middle, maximum trophic level TL_{max} (grey line), cut-off size L_{cut} (dashed line, in cm), mean species lengths $\overline{\overline{L}_m}$ (black line, on cm) compared to observations detailed in Fisher et al. (2010) (black dots) and species maximum size variability $\overline{\Delta L_m}$ (hatched, in cm) ; bottom, biomass production efficiency R^{Prod} (black line), residence time t_{Res} (grey line, in d).

3. Discussion

3.1. Latitudinal gradients

3.1.1. The species size gradient

Integrating individual bioenergetics and trophic interactions, the model predicts that the mean species size in fish communities $\overline{\overline{L}}_m$ increases with latitude (Fig. 8). This distribution evokes Bergmann's rule (Blackburn et al. (1999) ; Watt et al. (2010)), one of the most widespread biogeographical pattern. However, observed here for ectotherms it relies on different mechanisms, Bergmann's rule being formulated for endotherms.

High latitude ecosystems are characterized by high primary production levels (Fig. 3). Here high latitudes therefore support bigger consumer species (cf Fig. 6 left). Towards low latitude ecosystems are characterized by warmer temperatures. From the rich and cold pole to the poor and warm equator ecosystems, the warming decreases the attack rate of predators compared to their ingestion. Low latitudes favour the survival of smaller species (cf Fig. 6 right). With the present bioenergetics formulation the latitudinal distribution emerges from a balance between resource available and the capacity of fish to capture sufficient food.

For the simulated fish communities, the model predicts geometric mean maximum lengths $\overline{\overline{L}}_m$ in the same range of measurements compiled by Fisher et al. (2010). From bioenergetic considerations the model accounts for an observed increase in mean species length with increasing latitude, this shape remains consistent with variations of model parameters. However, other processes should also play a role on this distribution. For instance, we disregard the role of seasonality in the model and while at low latitude seasonal variations are small, at high latitude ecosystems are characterized by strong variations of their drivers (Fig. 3). Kooijman (2010) explains that large amplitude variations of primary producers supply in high latitudes ecosystems split the year into good and bad seasons. Bad seasons of poor food supply reduce populations, starting with the small species that have fewer reserves. Good seasons boost the development of

the surviving individuals enhancing the flux of energy toward larger populations. Seasonality would affect mid- to high latitude ecosystem properties. Moreover, we disregard the role of spatial interactions while movement may enhance the capacity of larger individuals to survive in resource limited areas. Using a spatially resolved spectrum model, Watson et al. (2015) show that in some ocean regions movement allows the survival of large predators and the emergence of expanded biomass spectra while stunted spectra were maintained without movement.

3.1.2. The gradient of species maximum size variability

The variability of species maximum size ($\overline{\Delta L_m}$) increases with latitude (Fig. 8). This is in agreement with the observation in Fisher et al. (2010) of an increased variability in species length as richness declines, when latitudes increase.

The model provides no measure of species richness, but the representation of the variability of species size accounts for the diversity of biomass pathways in the community. Rich and cold ecosystems maintain large species coexisting with small ones. They are characterized by high species size variability. In these ecosystems the energy derived from producers follows many different routes when it is consumed and moves up the food web. At low latitudes, the shrinking of the fish community reduces the range of possibilities. With less species size variability, these ecosystems offer less possible biomass pathways. The diversity of biomass pathways may impact the sensitivity of fish communities to environmental perturbations.

3.1.3. The maximum trophic level gradient

The maximum trophic level reached by fish communities at different latitudes is related to the maximum size of the individuals. Like the cut-off size L_{cut}, the maximum trophic level TL_{max} increases with latitude (Fig. 8). This result seems to contradict the observation of decreasing maximum trophic levels with latitude (Saporiti et al. (2015)). Three main hypotheses explain food chain lengths : the productivity hypothesis, more productive ecosystems should have longer food chain ; the dynamic stability hypothesis, food webs should be shorter in highly disturbed systems ; the species richness hypothesis, food chain

length increases with increasing species richness. The model simulates stable ecosystems, the dynamic stability hypothesis is not tested. The model disregards species richness, the species richness hypothesis is not tested. Therefore, the increase of the trophic chain length is consistent with the increase of low trophic level biomass with latitude, according to the productivity hypothesis, but more investigations are necessary.

The changes of the maximum trophic level are linked to the multi-stage response of communities to lower trophic level biomass and temperature variations (Fig. 6). At different latitudes it provides indications on the sensitivity of communities to environmental variations. Poor low latitude ecosystems of primary consumer are in the minimum trophic-length domain ($TL_{max} \simeq 2$), they are especially sensitive to variations (cf Fig. 6 left). Richer mid- to high latitude ecosystems support secondary consumers ($TL_{max} > 2$) exerting a top-down predation on primary consumers, they belong to the low or medium trophic-length domains and are more or less sensitive. High latitude saturated ecosystems ($TL_{max} \simeq 3$) are insensitive to variations. The phase diagram figure 7c with the superimposed mean environmental conditions along the latitudinal gradient summarizes this domains succession.

The phase diagram can be used to assess the impact of a global warming or global increase of lower trophic level biomass on the properties of ecosystems at different latitudes. For instance, a uniform warming would shift upward the distribution of latitudinal mean environmental conditions (see Fig. 7c). High latitude communities ($+/-60°$) would shift from a high to medium trophic-length domain with a decrease of fish biomass while lower latitudes ($+/-30°$) would shift from a low to minimum trophic-length domain. From pole to equator the fish community would be shrinking (Daufresne et al. (2009)). Similarly, a uniform increase of lower trophic level biomass would shift to the right the distribution of mean environmental conditions. From the equator to mid-latitudes ($+/-60°$), the fish community shifts through minimum, low and medium trophic-length domains indicating an increase of fish production compared to less sensitive saturated higher latitude ecosystems in the high trophic-length

domain.

3.2. Multi-stage response of fish production

3.2.1. Dependence on lower trophic level biomass

We identify four trophic-length domains : minimum, low, medium and high. In each of these, small-sized species survive and dominate larger size species because of their higher reproductive output. With increasing lower trophic level biomass, larger and larger species are sustained and trigger changes of domains, each characterized by interactions between primary producers, primary consumers and secondary consumers. Allowed by the explicit trait diversity representation in our model, our results underline the influence of trophic interactions on the link between primary production and fish biomass.

It should be noted that the appearing tri-trophic structure is directly linked to the definition of the size-selective predation in the model (Fig 4), especially the mean predator-prey mass ratio. A reduction of this ratio increases the length of the trophic chain. For instance, we tested (not shown) the relationship between lower trophic level biomass and fish biomass in a community reaching a trophic level of 4.5 and we obtained a similar succession of domains.

Moreover, the multi-domain response of fish communities relies on the coexistence of small and large species. In tri-trophic systems, the onset of intra-community predation has been shown to limit the coexistence of primary consumers with secondary ones (Mylius et al. (2001)). This property questions the commonness of omnivory and coexistence in marine ecosystems. Here, the density dependent schooling protects small species from depletion by predation and permits this coexistence, larger species develop leaning on smaller ones. Other models use alternative stabilizing factors such as additional resources, differential resource edibility or spatial and temporal refugees (Amarasekare (2007) ; Janssen et al. (2007)). Hartvig & Andersen (2013) justifies the existence of such trophic ladder state by a relationship between the ratio of sizes at maturation (or here maximum size) and the predator-prey mass ratio of interacting species.

Finally, the increase of fish biomass with increasing lower trophic level bio-

mass reaches a plateau towards the high trophic-length domain. This result may be a limit of the model definition on a finite range of individuals and species lengths. Another limit pointed by Jennings & Brander (2010) is a weakness of the size-spectrum representation which breaks down in larger size class because of the non linear relationship between trophic levels and body size for increasing species size. For example, filter feeding sharks and whales feed down the food chain. Therefore the formulation of the model with size-selective predation may not completely hold at high levels of lower trophic level biomass.

3.2.2. Dependence on temperature

The enhancement of metabolic rates with warming increases the energy demand and depending on the resource availability or assimilation efficiency, shifts in community properties occur (Petchey et al. (2010) ; O'Connor et al. (2009) ; Brose et al. (2012)). Here, we show that warming leads to an emergent shrinking of fish communities with multiple trophic-length domains (Fig 6 right) similar to those observed when changing lower trophic level biomass.

Both theoretical and empirical studies have shown that warming favours small species and lower trophic levels (Petchey et al. (2008, 2010)) over large bodied species in communities (Daufresne et al. (2009) ; Brose et al. (2012)). Here, this trend is reproduced and attributed to a difference of scaling with temperature of the energy assimilation that is scaling between T_{cor}^{q} and T_{cor}^{p} and energy dissipation that is scaling with T_{cor}. In our model, in order to maintain theoretical consistency $q = 1/3 < p = 1$, but there no consensus on these values (Rall et al. (2012) ; Englund et al. (2011)). Qualitatively, the behaviour of the model would be modified as follows if we could modify the relationship between p and q :

— $q = p = 1$: no dependence of the model to temperature, ingestion changes balance dissipation changes in any case.

— $p < q = 1$: with warming the ingestion increases less quickly than dissipation at high food density and at the same rate at low food density. The community shrinks and tends toward poor insensitive ecosystems.

— $p < q < 1$: with warming the ingestion increases less quickly than dissipation at high and low food densities. The community shrinks continuously.

Changes in the community structure due to warming are expected to impact the community characteristics. For example, Petchey et al. (2010) show that the relative dependence of handling time and attack rate to warming affects the connectance of food webs.

In the model, the impact of temperature on fish communities is weaker than the impact of lower trophic level biomass (Fig. 7a,b). But in real ecosystems, the sensitivity to temperature variations would be intensified by the impact of temperature on lower trophic levels. The dependence of marine ecosystems to temperature is therefore complex and we can expect fish community response to temperature and lower trophic level biomass variations to vary strongly with latitude (Brander (2007) ; Sarmiento et al. (2004)).

Conclusion

The present study investigates the response of fish communities to lower trophic level biomass and water temperature changes using a mechanistic DEB- and trait- based size-spectrum model (Maury & Poggiale (2013)). Parameterized for a generic fish community, the model is studied on a range of environmental conditions extracted from the outputs of a global physics and biochemistry model along a mean latitudinal gradient. The model reproduces the observed increase of geometric mean species length observed from the equator to the poles. Our results support the idea that bioenergetics and trophic processes strongly determine the structural and functional properties of communities. Moreover the model disentangles the impact of primary production from the impact of temperature on marine ecosystem's structure. We show that the different metabolism of small and large species and trophic interactions lead to a multi-domain response of communities to the environment.

This mechanistic model includes both individual's metabolism and predator-prey interactions to study the emergent structure, diversity and metabolism at the species and community levels. It relies on few parameters and represents the functional role of species diversity. It is useful for studying the impact of the environment in constant conditions, but the model also provides a sound basis to investigate other important structuring processes such as seasonality. In order to improve the realism of the present numerical experiments, the explicit consideration of spatial interactions could be also implemented in order to study the impact of environment in regional or global ecosystems (Cheung et al. (2010) ; Blanchard et al. (2012) ; Brander (2010) ; Watson et al. (2015) ; Lefort et al. (2015)). Finally, other environmental stressors could be tested, such as the effect of acidification (Fabry et al. (2008)) and oxygen limitation (Prtner & Knust (2007)), or constraints such as thermal ranges (Englund et al. (2011)).

Acknowledgment

This study was supported by the ANR project MACROES (MACRoscope for Oceanic Earth System ANR-09-CEP-003)

Rfrences

Amarasekare, P. (2007). Trade-offs, temporal variation, and species coexistence in communities with intraguild predation. *Ecology*, *88*, 2720–2728.

Andersen, K. H., & Beyer, J. E. (2006). Asymptotic size determines species abundance in the marine size spectrum. *The American Naturalist*, *168*, 54–61.

Aumont, O., Ethé, C., Tagliabue, A., Bopp, L., & Gehlen, M. (2015). Pisces-v2 : an ocean biogeochemical model for carbon and ecosystem studies. *Geoscientific Model Development*, *8*, 2465–2513.

Benoît, E., & Rochet, M.-J. (2004). A continuous model of biomass size spectra governed by predation and the effects of fishing on them. *Journal of theoretical Biology*, *226*, 9–21.

Bindoff, N., Willebrand, J., Artale, V., Cazenave, A., Gregory, J., Gulev, S., Hanawa, C., K.and Le Qur, Levitus, S., Nojiri, Y., Shum, C., L.D., T., & ., U. A. (2007). *Observations : Oceanic Climate Change and Sea Level. In : Climate Change 2007 : The Physical Science Basis. Contribution of Working Group I to the Fourth Assessment Report of the Intergovernmental Panel on Climate Change [Solomon, S., D. Qin, M. Manning, Z. Chen, M. Marquis, K.B. Averyt, M. Tignor and H.L. Miller (eds.)]*. Cambridge University Press, Cambridge, United Kingdom and New York, NY, USA.

Blackburn, T. M., Gaston, K. J., & Loder, N. (1999). Geographic gradients in body size : a clarification of bergmann's rule. *Diversity and Distributions*, *5*, 165–174.

Blanchard, J. L., Jennings, S., Holmes, R., Harle, J., Merino, G., Allen, J. I., Holt, J., Dulvy, N. K., & Barange, M. (2012). Potential consequences of climate change for primary production and fish production in large marine ecosystems. *Philosophical Transactions of the Royal Society of London B : Biological Sciences*, *367*, 2979–2989.

Blanchard, J. L., Jennings, S., Law, R., Castle, M. D., McCloghrie, P., Rochet, M.-J., & Benot, E. (2009). How does abundance scale with body size in coupled size-structured food webs ? *Journal of Animal Ecology*, *78*, 270–280.

Bopp, L., Resplandy, L., Orr, J. C., Doney, S. C., Dunne, J. P., Gehlen, M., Halloran, P., Heinze, C., Ilyina, T., Séférian, R., Tjiputra, J., & Vichi, M. (2013). Multiple stressors of ocean ecosystems in the 21st century : projections with cmip5 models. *Biogeosciences*, *10*, 6225–6245.

Brander, K. M. (2007). Global fish production and climate change. *Proceedings of the National Academy of Sciences*, *104*, 19709–19714.

Brander, K. M. (2010). Impacts of climate change on fisheries. *Journal of Marine Systems*, *79*, 389 – 402.

Brose, U., Dunne, J. A., Montoya, J. M., Petchey, O. L., Schneider, F. D., & Jacob, U. (2012). Climate change in size-structured ecosystems. *Philosophical Transactions of the Royal Society of London B : Biological Sciences*, *367*, 2903–2912.

Cheung, W. W. L., Lam, V. W. Y., Sarmiento, J. L., Kearney, K., Watson, R., & Pauly, D. (2009). Projecting global marine biodiversity impacts under climate change scenarios. *Fish and Fisheries*, *10*, 235–251.

Cheung, W. W. L., Lam, V. W. Y., Sarmiento, J. L., Kearney, K., Watson, R., Zeller, D., & Pauly, D. (2010). Large-scale redistribution of maximum fisheries catch potential in the global ocean under climate change. *Global Change Biology*, *16*, 24–35.

Clarke, A., & Fraser, K. P. P. (2004). Why does metabolism scale with temperature ? *Functional Ecology*, *18*, 243–251.

Clarke, A., & Johnston, N. M. (1999). Scaling of metabolic rate with body mass and temperature in teleost fish. *Journal of Animal Ecology*, *68*, 893–905.

Daufresne, M., Lengfellner, K., & Sommer, U. (2009). Global warming benefits the small in aquatic ecosystems. *Proceedings of the National Academy of Sciences*, *106*, 12788–12793.

De Roos, A. M., & Persson, L. (2001). Physiologically structured models from versatile technique to ecological theory. *Oikos*, *94*, 51–71.

De Roos, A. M., & Persson, L. (2013). *Population and community ecology of ontogenetic development*. Princeton University Press.

Doney, S. C., Ruckelshaus, M., Emmett Duffy, J., Barry, J. P., Chan, F., English, C. A., Galindo, H. M., Grebmeier, J. M., Hollowed, A. B., Knowlton, N., Polovina, J., Rabalais, N. N., Sydeman, W. J., & Talley, L. D. (2012). Climate change impacts on marine ecosystems. *Annual Review of Marine Science*, *4*, 11–37.

Dueri, S., Bopp, L., & Maury, O. (2014). Projecting the impacts of climate change on skipjack tuna abundance and spatial distribution. *Global Change Biology*, *20*, 742–753.

Englund, G., hlund, G., Hein, C. L., & Diehl, S. (2011). Temperature dependence of the functional response. *Ecology Letters*, *14*, 914–921.

Fabry, V. J., Seibel, B. A., Feely, R. A., & Orr, J. C. (2008). Impacts of ocean acidification on marine fauna and ecosystem processes. *ICES Journal of Marine Science : Journal du Conseil*, *65*, 414–432.

Fisher, J. A. D., Frank, K. T., & Leggett, W. C. (2010). Global variation in marine fish body size and its role in biodiversity-ecosystem functioning. *Marine Ecology Progress Series*, *405*, 1–13.

Fulton, E. A., CSIRO, & Authority, A. F. M. (2004). *Ecological indicators of the ecosystem effects of fishing : final report*. Hobart : CSIRO ; Canberra : Australian Fisheries Management Authority. "Report Number R99/1546".

Gillooly, J. F., Brown, J. H., West, G. B., Savage, V. M., & Charnov, E. L. (2001). Effects of size and temperature on metabolic rate. *Science*, *293*, 2248–2251.

Grimm, V. (1999). Ten years of individual-based modelling in ecology : what have we learned and what could we learn in the future ? *Ecological Modelling*, *115*, 129 – 148.

Hartvig, M., & Andersen, K. H. (2013). Coexistence of structured populations with size-based prey selection. *Theoretical Population Biology*, *89*, 24 – 33.

Hartvig, M., Andersen, K. H., & Beyer, J. E. (2011). Food web framework for size-structured populations. *Journal of Theoretical Biology*, *272*, 113 – 122.

Holling, C. S. (1959). Some characteristics of simple types of predation and parasitism. *The Canadian Entomologist*, *91*, 385–398.

Janssen, A., Sabelis, M. W., Magalhães, S., Montserrat, M., & Van der Hammen, T. (2007). Habitat structure affects intraguild predation. *Ecology*, *88*, 2713–2719.

Jennings, S., & Brander, K. (2010). Predicting the effects of climate change on marine communities and the consequences for fisheries. *Journal of Marine Systems*, *79*, 418–426.

Kooijman, S. A. L. M. (2000). *Dynamic Energy and Mass Budgets in Biological Systems*. (2nd ed.). Cambridge University Press. Cambridge Books Online.

Kooijman, S. A. L. M. (2010). *Dynamic Energy and Mass Budgets in Biological Systems*. (3rd ed.). Cambridge University Press. Cambridge Books Online.

Kooijman, S. A. L. M., & Lika, K. (2014). Comparative energetics of the 5 fish classes on the basis of dynamic energy budgets. *Journal of Sea Research*, *94*, 19–28.

Lefort, S., Aumont, O., Bopp, L., Arsouze, T., Gehlen, M., & Maury, O. (2015). Spatial and body-size dependent response of marine pelagic communities to projected global climate change. *Global Change Biology*, *21*, 154–164.

Lehodey, P., Senina, I., & Murtugudde, R. (2008). A spatial ecosystem and populations dynamics model (seapodym) modeling of tuna and tuna-like populations. *Progress in Oceanography*, *78*, 304 – 318.

Lika, K., Kearney, M. R., Freitas, V., van der Veer, H. W., van der Meer, J., Wijsman, J. W. M., Pecquerie, L., & Kooijman, S. A. L. M. (2011). The covariation method for estimating the parameters of the standard dynamic energy budget model i : Philosophy and approach. *Journal of Sea Research*, *66*, 270 – 277. The AquaDEB project (phase II) : what we've learned from applying the Dynamic Energy Budget theory on aquatic organisms.

Maury, O., & Poggiale, J.-C. (2013). From individuals to populations to communities : A dynamic energy budget model of marine ecosystem size-spectrum including life history diversity. *Journal of Theoretical Biology*, *324*, 52 – 71.

Maury, O., Shin, Y.-J., Faugeras, B., Ari, T. B., & Marsac, F. (2007). Modeling environmental effects on the size-structured energy flow through marine ecosystems. part 2 : Simulations. *Progress in Oceanography*, *74*, 500 – 514.

Merino, G., Barange, M., Blanchard, J. L., Harle, J., Holmes, R., Allen, I., Allison, E. H., Badjeck, M. C., Dulvy, N. K., Holt, J., Jennings, S., Mullon, C., & Rodwell, L. D. (2012). Can marine fisheries and aquaculture meet fish demand from a growing human population in a changing climate ? *Global Environmental Change*, *22*, 795 – 806.

Metz, J. A., & Diekmann, O. (1986). The dynamics of physiologically structured populations. *Lecture notes in biomathematics*, *68*.

Mylius, S. D., Klumpers, K., de Roos, A. M., & Persson, L. (2001). Impact of intraguild predation and stage structure on simple communities along a productivity gradient. *The American Naturalist*, *158*, 259–276.

O'Connor, M. I., Piehler, M. F., Leech, D. M., Anton, A., Bruno, J. F., & Loreau, M. (2009). Warming and resource availability shift food web structure and metabolism. *PLoS Biology*, *7*.

Petchey, O. L., Beckerman, A. P., Riede, J. O., & Warren, P. H. (2008). Size, foraging, and food web structure. *Proceedings of the National Academy of Sciences*, *105*, 4191–4196.

Petchey, O. L., Brose, U., & Rall, B. C. (2010). Predicting the effects of temperature on food web connectance. *Philosophical Transactions of the Royal Society of London B : Biological Sciences*, *365*, 2081–2091.

Peterson, A. T. (2003). Predicting the geography of species invasions via ecological niche modeling. *The Quarterly Review of Biology*, *78*, 419–433.

Prtner, H. O., & Knust, R. (2007). Climate change affects marine fishes through the oxygen limitation of thermal tolerance. *Science*, *315*, 95–97.

Rall, B. C., Brose, U., Hartvig, M., Kalinkat, G., Schwarzmüller, F., Vucic-Pestic, O., & Petchey, O. L. (2012). Universal temperature and body-mass scaling of feeding rates. *Philosophical Transactions of the Royal Society of London B : Biological Sciences*, *367*, 2923–2934.

Rice, J. C., & Garcia, S. M. (2011). Fisheries, food security, climate change, and biodiversity : characteristics of the sector and perspectives on emerging issues. *ICES Journal of Marine Science : Journal du Conseil*, .

Saporiti, F., Bearhop, S., Vales, D. G., Silva, L., Zenteno, L., Tavares, M., Crespo, E. A., & Cardona, L. (2015). Latitudinal changes in the structure of marine food webs in the southwestern atlantic ocean. *Marine Ecology Progress Series*, *538*, 23.

Sarmiento, J. L., Slater, R., Barber, R., Bopp, L., Doney, S. C., Hirst, A. C., Kleypas, J., Matear, R., Mikolajewicz, U., Monfray, P., Soldatov, V., Spall, S. A., & Stouffer, R. (2004). Response of ocean ecosystems to climate warming. *Global Biogeochemical Cycles*, *18*, n/a–n/a.

Scharf, F. S., Juanes, F., & Rountree, R. A. (2000). Predator size-prey size relationships of marine fish predators : interspecific variation and effects of ontogeny and body size on trophic-niche breadth. *Marine Ecology Progress Series*, *208*, 229–248.

Sheldon, R. W., Prakash, A., & Sutcliffe, W. H. (1972). The Size Distribution of Particles in the Ocean. *Limnology and Oceanography*, *17*, 327–340.

Sheridan, J. A., & Bickford, D. (2011). Shrinking body size as an ecological response to climate change. *Nature Clim. Change*, *1*, 401–406.

Shin, Y. J., & Cury, P. (2001). Exploring fish community dynamics through size-dependent trophic interactions using a spatialized individual-based model. *Aquatic Living Resources*, *14*, 65–80.

Shin, Y.-J., Rochet, M.-J., Jennings, S., Field, J. G., & Gislason, H. (2005). Using size-based indicators to evaluate the ecosystem effects of fishing. *ICES Journal of Marine Science : Journal du Conseil*, *62*, 384–396.

Watson, J. R., Stock, C. A., & Sarmiento, J. L. (2015). Exploring the role of movement in determining the global distribution of marine biomass using a coupled hydrodynamic size-based ecosystem model. *Progress in Oceanography*, *138, Part B*, 521 – 532.

Watt, C., Mitchell, S., & Salewski, V. (2010). Bergmann's rule ; a concept cluster ? *Oikos*, *119*, 89–100.

Woodworth-Jefcoats, P. A., Polovina, J. J., Dunne, J. P., & Blanchard, J. L. (2013). Ecosystem size structure response to 21st century climate projection : large fish abundance decreases in the central north pacific and increases in the california current. *Global Change Biology*, *19*, 724–733.

Appendix A : Dynamic Energy Budget at individual level

TABLE 3 : DEB energy flux as a function of primary DEB parameters, the energy reserve E, the structural volume V, for an individual of a given maximum species length V_m (Kooijman (2000, 2010)). T_{cor} expresses the temperature correction of metabolic activity.

Eq. No.	**Metabolic process**	**Energy flux (in Jd^{-1})**
T3.a	Ingestion	$\dot{p}_X^{V_m} = \{\dot{p}_{Xm}^{V_m}\} f_V^{V_m} V^{2/3} T_{cor}$
T3.b	Assimilation	$\dot{p}_A^{V_m} = \kappa_X \dot{p}_X^{V_m} T_{cor} = \dot{p}_{Am_{max}}^{V_m} f_V^{V_m} T_{cor} = \{\dot{p}_{Am}^{V_m}\} f_V^{V_m} V^{2/3} T_{cor}$
T3.c	Catabolism	$\dot{p}_C^{V_m} = \frac{f_V^{V_m}[E_m]}{[E_G]+\kappa f_V^{V_m}[E_m]} \quad [E_G]\nu V^{2/3} + [\dot{p}_M] V \quad T_{cor}$
T3.d	Reserve growth	$\dot{p}_E^{V_m} = \dot{p}_A^{V_m} - \dot{p}_C^{V_m}$
T3.e	Structural maintenance	$\dot{p}_M^{V_m} = [\dot{p}_M] V T_{cor}$
T3.f	Structural growth	$\dot{p}_G^{V_m} = \kappa \dot{p}_C^{V_m} - \dot{p}_M^{V_m}$
T3.g	Maturity maintenance	$\dot{p}_J^{V_m} = \frac{1-\kappa}{\kappa}[\dot{p}_M] min \quad V, V_p^{V_m} \quad T_{cor}$
T3.h	Reproduction	$\dot{p}_R^{V_m} = (1-\kappa)\, \dot{p}_C^{V_m} - \dot{p}_J^{V_m}$

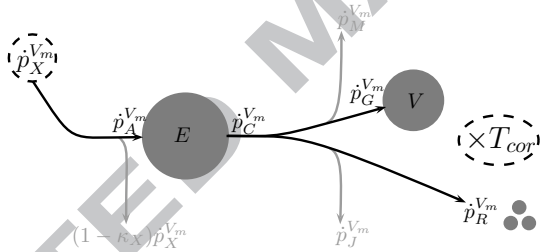

FIGURE 9 : Schematic representation of the DEB state variables (compartments) and energy flow (arrows) involved in the bioenergetics of any individual of a species of maximum volume V_m : in black energy flux linked to the species and community levels ; in grey energy flux lost or dissipated. The environment impacts individuals through variations of food density and body temperature (dashed) and influences the dynamic of the emerging community.

Appendix B : Abundance spectra at species and community levels

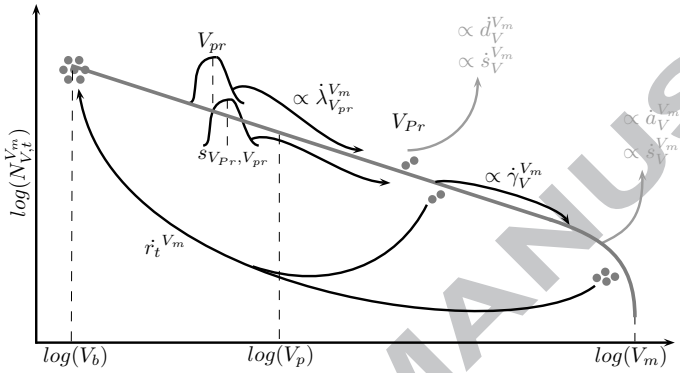

(a) Species : species abundance size-spectrum (black line) emerging form the advection of individuals along structural volumes driven by size-selective predation and individual level bioenergetics, for a species of maximum volume V_m.

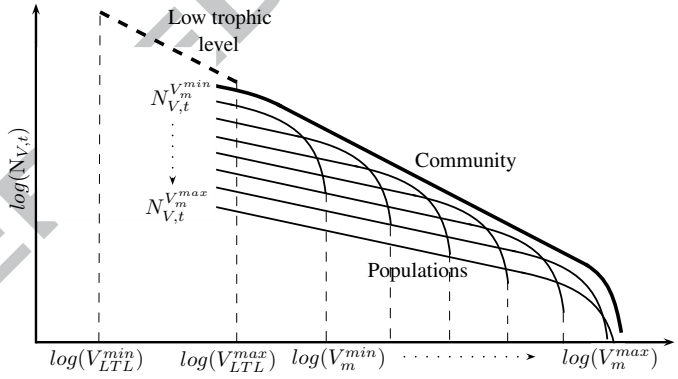

(b) Community : community size-spectrum (black line) as integral of species spectra (thin black lines) of asymptotic volume V_m.

FIGURE 10 : Schematic representation of the energy flow (arrows) at species level and emergent community spectrum level on the range of structural volumes $V \in [V_b, V_m^{max}]$: in black energy flux allowing the emergence of the community ; in grey energy flux lost or dissipated. The individual level response to perturbations affects the species level dynamic and the emergent community features.

TABLE 4 : Summary of model's governing equations (Maury & Poggiale (2013)). T_{cor} express the temperature correction. $[x]^+ = x$ if $x > 0$, 0 else.

Eq.	Process	Equation
Consumers governing equations		
T4.a	Species dynamics equation ($\forall\ V_m$)	$\frac{\partial N_{V,t}^{V_m}}{\partial t} = -\frac{\partial(\gamma_{V,t}^{V_m} N_{V,t}^{V_m})}{\partial V} - (\dot{\lambda}_{V,t}^{V_m} + \dot{a}_{V,t}^{V_m} + \dot{d}_{V,t}^{V_m} + \dot{s}_{V,t}^{V_m}) N_{V,t}^{V_m}$
T4.b	Birth abundance flux (at $V = V_b$)	$\gamma_{V_b,t}^{V_m} N_{V_b,t}^{V_m} = \dot{r}_t^{V_m}$
T4.c	Community abundance distribution	$\mathrm{N}_{V,t} = \int_{V_m} N_{V,t}^{V_m}\, dV_m$
T4.d	Equivalence energy/abundance	$\xi_{V,t}^{V_m} = (E^* + d\psi V) N_{V,t}^{V_m}$
T4.e	Reserve energy	$E^* = f_{V,t}^{V_m} [E_m^{V_m}] V$
Food encounter		
T4.f	Predator size-selectivity on prey	$s_{V,U} = \frac{1 - \ 1+exp\ \ \alpha_2\ \ \rho_2 - \left(\frac{V}{U}\right)^{1/3}\ \ ^{-1}}{1+exp\ \ \alpha_1\ \ \rho_1 - \left(\frac{V}{U}\right)^{1/3}}$
T4.g	Schooling probability	$ps_{V,t}^{V_m} = \frac{(V\xi_{V,t}^{V_m})^\beta}{s_{cr}^\beta + (V\xi_{V,t}^{V_m})^\beta}$
Predation		
T4.h	Energy content of available prey	$p_{V,t} = p_{V,t}^C + p_{V,t}^{LTL}$
T4.i	Prey density of consumers	$p_{V,t}^C = \int_{U=V_b}^{V_m^{max}} s_{V,U} \left(\int_{V_m=U}^{V_m^{max}} ps_{U,t}^{V_m} \xi_{U,t}^{V_m}\, dV_m \right) dU$
T4.j	Prey density of low trophic levels	$p_{V,t}^{LTL} = \int_{U=V_{ltl}^{min}}^{U=V_{ltl}^{max}} s_{V,U} \xi_{U,t}^{ltl} dU$
T4.k	Holling type II functional response	$f_{V,t}^{V_m} = \frac{p_{V,t}}{C' V_m^{1/3} V^{-1/3} T_{cor}^{p-q} + p_{V,t}}$
Growth		
T4.l	Instantaneous growth rate	$\dot{\gamma}_{V,t}^{V_m} = \frac{[\dot{p}_G^{V_m}]^+}{[E_G]}$
Mortality		
T4.m	Starvation mortality coefficient	$\dot{s}_{V,t}^{V_m} = \frac{N_{V,t}^{V_m}}{\xi_{V,t}^{V_m}}\ \ [-\dot{p}_G^{V_m}]^+ + [-\dot{p}_R^{V_m}]^+$
T4.n	Disease mortality coefficient	$\dot{d}_{V,t}^{V_m} = D\ ps_{V,t}^{V_m} T_{cor}$
T4.o	Ageing mortality coefficient	$\dot{a}_{V,t}^{V_m} = \frac{\ddot{h}_a}{V_t} \int_{t_1=0}^{t_1=t} V_{t_1}\, dt_1 - V_b t + \frac{[\dot{p}_M]}{[E_G]} \int_{t_1=0}^{t_1=t} \int_{t_2=0}^{t_2=t_1} V_{t_2}\, dt_2 dt_1$
T4.p	Predation mortality coefficient	$\dot{\lambda}_{V,t}^{V_m} = \frac{ps_{V,t}^{V_m}}{\kappa_X} \int_{V_m=V_b}^{V_m^{max}} \int_{U=V_b}^{V_m} \frac{\{\dot{p}_{Am}\} \xi_{U,t}^{V_m} U^{-1/3} s_{V,U} f_{V,t}^{V_m}}{p_{U,t}(d\psi + E^*/V)}\ \ dU dV_m$
Reproduction		
T4.q	Reproductive input	$\dot{r}_t^{V_m} = (1 - M_{egg}) \phi \kappa_R \int_{V_p}^{V_m} N_{V,t}^{V_m} [\dot{p}_R^{V_m}]^+ dV$
Temperature		
T4.r	Arrhenius correction	$\dot{\rho}(T) = \dot{\rho}(T_{ref}) exp\ \ \frac{T_A}{T_{ref}} - \frac{T_A}{T}\ \ = \dot{\rho}(T_{ref}) T_{cor}$

Appendix C : Community level energy balance

The community size-spectrum can be visualized as a compartment which draws its resource from the lower trophic levels, through size-selective predation, and loses it through individual level dissipation, disease or ageing mortality, growth overhead or fecundation loss (see Fig.11). The model being energy balanced from individuals to species to the community, at stationary steady state the input of energy $\dot{P}_{in} = \dot{P}_{PP,t}$ rigorously balances the output $\dot{P}_{out} = \dot{P}_{Dissip,t} + \dot{P}_{Loss,t}$, i.e. $\dot{P}_{in} = \dot{P}_{out}$.

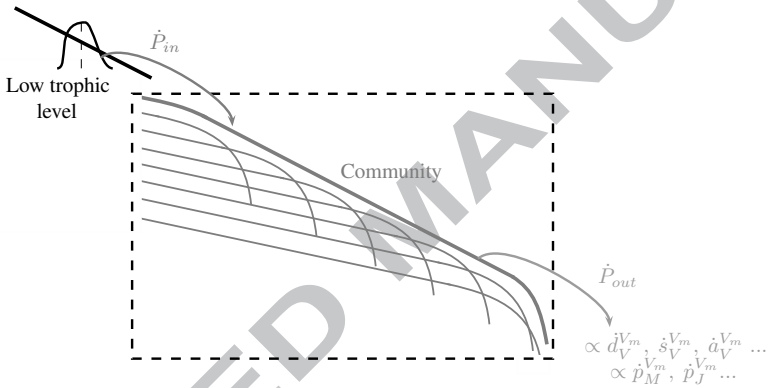

FIGURE 11 : Community level energy balance at stationary steady state.

Appendix D : DEB fish parameters

In Kooijman (2010), a set of generic DEB parameters are provided. While the present model in its initial formulation used these values (Maury & Poggiale (2013)), we here adapted them to better account for fish communities.

— **Volume specific cost of growth** $[E_G]$ **:** The ash-free-dry-weight of fish is taken higher $d_{V_{dry}} = 0.2\ g\ cm^{-3}$ (against $d_{V_{dry}} = 0.1\ g\ cm^{-3}$ for the generic parameters) for a wet mass at $d_{V_{wet}} = 1\ g\ cm^{-3}$ (Lika et al. (2011)). With a chemical potential for structure of $\mu_V = 560\ kJ\ Cmol^{-1}$, a growth efficiency of $\kappa_G = 0.8$ and a dry molecular weight for structure taken $w_{V_{dry}} = 24.6\ g\ C - mol^{-1}$:

$$[E_G] = \frac{\mu_V \frac{d_{V_{dry}}}{w_V}}{\kappa_G} = 5691\ J\ cm^{-3} \tag{12}$$

— **Energy content of biomass** Ψ **:** We assumed identical chemical potentials for structure and reserve, $\mu_E = \mu_V = 560\ kJ\ Cmol^{-1}$, identical molecular weights for structure and reserve $w_{E_{dry}} = w_{V_{dry}} = 24.6\ g\ C - mol^{-1}$, $w_{E_{wet}} = w_{V_{wet}} = w_{*_{dry}}/0.2$:

$$\Psi = \frac{\mu_*}{w_{*_{wet}}} = 4552J\ g^{-1} \tag{13}$$

Kooijman & Lika (2014) compile the DEB parameters specific of fish communities, we adapt the generic parameters.

— **Somatic maintenance rate** $[\dot{p}_M] = 25\ J\ d^{-1}cm^{-3}$ **:** Due to this modification the **maximum surface-specific assimilation rate** becomes proportional to $\alpha_{\{\dot{p}_{Am}\}} = 31.25\ J\ cm^{-3}\ d^{-1}$.

— **The structural volume at puberty** $V_p = \alpha_p V_m$**,** $\alpha_p = 0.125$ **:** For all fish it is estimated that $L_p = 0.5L_m$, $V_p = 0.125V_m$.

The **maximum reserve density** has been corrected to better fit empirical growth curves, $\alpha_{[E_m]} = 312.5\ J\ cm^{-4}$ which induces an **energy conductance** $\nu = 0.1$.

We use a DEB-, trait-based community size-spectrum model to assess the impact of low trophic level's biomass and temperature on fish communities at steady state.

Multiple domains with different sensitivities to environmental changes are observed. They are linked to the number of trophic levels sustained in communities.

Differences in the scaling of individual's metabolism and prey assimilation with temperature lead to a shrinking of fish communities with warming.

The model explains why larger species compose fish communities when latitude increases.